ChemPubSoc Europe

DOI: 10.1002/cmdc.201402555

CHEMMEDCHEM Full Papers

Fluorine in Drug Design: A Case Study with Fluoroanisoles

Li Xing,*[a] David C. Blakemore,[b] Arjun Narayanan,[a] Ray Unwalla,[a] Frank Lovering,[a] R. Aldrin Denny,[a] Huanyu Zhou,[c] and Mark E. Bunnage[a]

Anisole and fluoroanisoles display distinct conformational preferences, as evident from a survey of their crystal structures. In addition to altering the free ligand conformation, various degrees of fluorination have a strong impact on physicochemical and pharmacokinetic properties. Analysis of anisole and fluoroanisole matched molecular pairs in the Pfizer corporate database reveals interesting trends: 1) $PhOCF_3$ increases log *D* by ~1 log unit over $PhOCH_3$ compounds; 2) $PhOCF_3$ shows lower passive permeability despite its higher lipophilicity; and 3) $PhOCF_3$ does not appreciably improve metabolic stability over $PhOCH_3$. Emerging from the investigation, difluoroanisole ($PhOCF_2H$) strikes a better balance of properties with noticeable advantages of log *D* and transcellular permeability over $PhOCF_3$. Synthetic assessment illustrates that the routes to access difluoroanisoles are often more straightforward than those for trifluoroanisoles. Whereas replacing $PhOCH_3$ with $PhOCF_3$ is a common tactic to optimize ADME properties, our analysis suggests $PhOCF_2H$ may be a more attractive alternative, and greater exploitation of this motif is recommended.

Introduction

Fluorine is an often-used substituent in drug design owing to its unique combination of electronegativity, size, and lipophilicity, and much has been learned about its interactions with protein targets.[1] Introduction of fluorine into a small molecule can be used to replace interactions of undesired functionalities or to form novel interactions unavailable to the parent species. For example, while fluorine is not a good hydrogen bond acceptor, it is able to support hydrogen bonding interactions, with a recent study showing that the propensity of alkyl fluorides to engage in hydrogen bonds is lower than acetophenone following the order of $CFH_2 > CF_2H > CF_3$.[2] Furthermore, the high electronegativity of the fluorine atom allows C–F bonds to form dipolar and multipolar interactions with protein backbone or side-chain amide groups, or with the pi-face of the guanidinium group of arginine.[3] This has led to the identification of fluorophilic protein environments that can be targeted in a rational manner by structure-based drug design.[3b,c,4]

While fluorine can provide unique protein-ligand interactions, the optimization of small molecule ligands into drug candidates requires the balance of potency with physicochemical and pharmacokinetic properties. Due to the increased bond strength of the C–F bond relative to the C–H bond, replacement of hydrogen with fluorine has been a medicinal chemistry strategy for decreasing cytochrome P450 (CYP)-mediated metabolism for many years, with numerous examples of success.[5] Fluorine can decrease metabolism either directly, by blocking the site of modification, or indirectly, by altering the electronics near the metabolism site. However, depending on the impact of the addition of fluorine on overall molecular properties, such as increased lipophilicity,[6] and the electronic and spatial relationship of the site of fluorination to the site of metabolism, the rate of CYP-mediated oxidation can be either decreased or enhanced.[7]

The increased size and electronegativity of fluorine relative to hydrogen can have a substantial impact on molecular conformation, which can affect the binding affinity to a target by altering the energy required for the ligand to reorganize into its binding conformation. This conformational effect is well exemplified when comparing anisole, in which the methoxy group prefers to be in-plane with the phenyl ring, with trifluoroanisole, in which the trifluoromethoxy group exhibits a strong preference to be out of plane.[1a,6,8] Intermediate states of fluorination decrease the in-plane preference observed in anisole.[1a]

Whereas anisole ($PhOCH_3$) and trifluoroanisole ($PhOCF_3$) are well-explored moieties in medicinal chemistry programs, $PhOCFH_2$ and $PhOCF_2H$ are much less used. Nonetheless we found four difluoroanisole-containing drug molecules on the market, namely garenoxacin, pantoprazole, roflumilast and riodipine (Figure 1), and additionally 17 molecules currently under investigation in the clinical setting (Supporting Information, Figure S1). As part of a general interest in the use of fluorine atom in drug design, we were curious to explore the properties of fluorinated anisoles relative to anisoles and determine the influence of fluorination on properties such as lipophilicity, metabolic stability and permeability. Herein we present results from a systematic analysis of matched molecular pairs (MMPs) of anisole- and fluoroanisole-containing compounds from the

[a] *L. Xing, A. Narayanan, R. Unwalla, F. Lovering, R. A. Denny, M. E. Bunnage*
Worldwide Medicinal Chemistry, Pfizer Inc., Cambridge, MA (USA)
E-mail: li.xing@pfizer.com

[b] *D. C. Blakemore*
Worldwide Medicinal Chemistry, Pfizer Neusentis, Cambridge (UK)

[c] *H. Zhou*
Biotherapeutics Clinical Research, Pfizer Inc., Cambridge, MA (USA)

Supporting information for this article is available on the WWW under http://dx.doi.org/10.1002/cmdc.201402555.

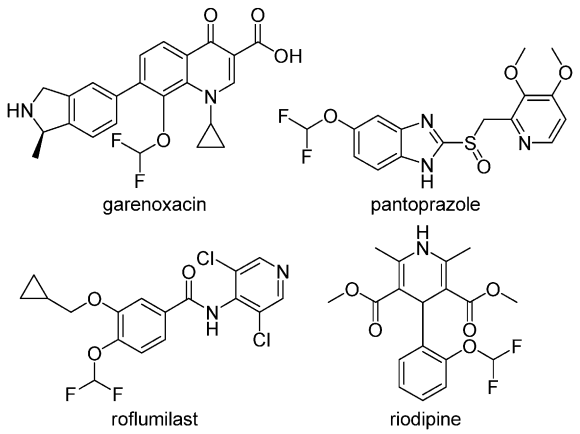

Figure 1. Marketed drugs that contain the difluoroanizole substructure.

Pfizer in-house database, which suggest that $PhOCF_2H$ may provide distinct advantages over $PhOCF_3$ in optimization of ADME properties. Some representative examples of matched molecular pairs from this data set are shown in Figure 2 for illustrative purposes. Whereas the trifluoromethoxy compound **2** has an increased HLM clearance and lower RRCK relative to its methoxy MMP **1**, the difluoromethoxy compound **3** shows lower HLM clearance and higher RRCK over its trifluoromethoxy MMP **4**. The systematic analysis of MMPs described herein explores the generality of such trends.

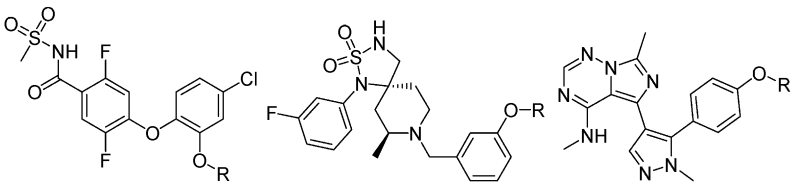

	1	2	3	4	5	6
R	CH_3	CF_3	CF_2H	CF_3	CF_2H	CH_3
HLM [mL min^{-1} mg^{-1}][a]	49.5	81.8	36	>320	<8.0	11.4
RRCK [10^{-6} cm s^{-1}][b]	12.5	7.1	20.9	7.0	29.1	17.9

[a] Human liver microsomal clearance. [b] Ralph Russ canine kidney cell line permeability.

Figure 2. Representative matched molecular pairs.

Results and Discussion

Conformational analysis

Although anisole fluorination is most commonly explored as a tactic to optimize ADME properties, we were also interested to understand the impact of fluorination on free ligand conformation, as this influences the extent to which fluoroanisoles can be considered as anisole bioisosteres from a target-binding perspective. We thus began our study with a systematic analysis of anisole and fluoroanisole conformations.

Thousands of examples were retrieved from the CSD for $PhOCH_3$, which clearly shows discrete peaks at 0 and 180° in the frequency histogram (Figure 3a). To avoid conformational bias imposed by steric constraints, all substructural queries were constructed such that at least one *ortho*-position of the anisoles remains unsubstituted. The preference is remarkably strong for the methoxy to be in the same plane with the aromatic ring system. In contrast to the coplanar state of $PhOCH_3$, the trifluoromethoxy predominantly adopts an orthogonal conformation to the phenyl ring, as indicated by the principal distribution at ±90° (Figure 3c). Figure 3b shows the torsional profile of the $PhOCF_2H$ group, which apparently spreads over a large range without any distinct orientational preference. It is noted there are only 22 data points for $PhOCF_2H$, much less

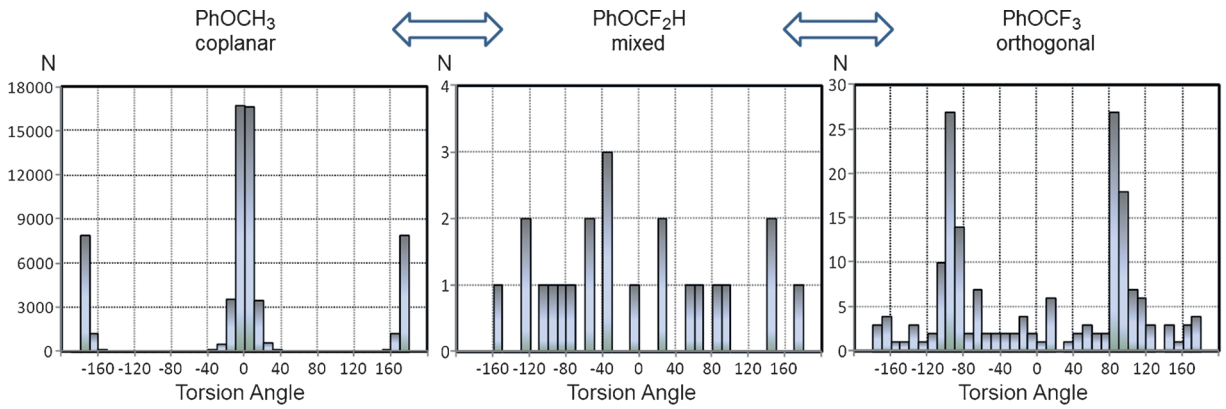

Figure 3. Torsional profiles retrieved from CSD. Apparent is the transition of conformational preference from $PhOCH_3$ (coplanar) through $PhOCF_2H$ (mixed) to $PhOCF_3$ (orthogonal).

than the number of examples for $PhOCH_3$ and $PhOCF_3$. Further examination of these X-ray structures shows there is no preference for the other torsion angle that is, C(ar)-O-C-F. In all of the observed C(ar)-C(ar)-O-C torsions, existence of either both or one C–F bond is observed in an anomeric orientation that is, C(ar)-O-C-F torsion ~60°. This is nicely borne out by the $PhOCF_2H$ CSD structures that is, ZIJFAB and SOTBAE (Figure S2). Both have an approximate orthogonal conformation (81 and 89°) with respect to the C(ar)-C(ar)-O-C torsion. However, the SOTBAE entry has both C–F bonds in an anomeric orientation (*endo-endo* conformation), while only one anomeric C–F bond is observed for ZIJFAB (*endo-exo* conformation). No examples of crystal structures were found for $PhOCFH_2$.

This is a case where strong steric and electronic effects of fluorine substitution fundamentally shift the conformational preference. In anisole, the stabilizing mesomeric interaction between the phenyl electrons and the oxygen lone pair is predominant, which is maximized at the coplanar conformation. On the other hand, the high electronegativity of fluorine results in a highly polarized C–F bond, and a vacant low-energy σ^* orbital of the O–CF_3 bond that can interact with the adjacent σ bonds or nonbonding electron pairs. A comparison between anisole and trifluoroanisole illustrates the interplay between the resonance and inductive effect. The orientation of the methyl group relative to the benzene plane results from the balance of the two opposing effects: 1) resonance effects that favor the coplanar conformation to maximize the electronic conjugation between the oxygen lone pairs and the aromatic π system; 2) counteracting steric effects that favor the orthogonal conformation due to steric repulsion with the ortho hydrogen atoms on the phenyl ring. Because of the strong electron-withdrawing property of the trifluoromethyl group, the resonance donor capacity is attenuated and in part balanced by the overlap between the phenyl π-orbital and the σ^* orbital, resulting in reduced conjugation with the aromatic ring. Furthermore, the additional steric bulk of the trifluoromethoxy group increases the effects of sterics on conformation. In combination, the decrease in the resonance effect and the increase in the steric effect both contribute to the orthogonal conformation observed for $PhOCF_3$. Quantum mechanics calculations have produced the corresponding energy minima for $PhOCH_3$ and $PhOCF_3$. Using theories and basis sets of different levels and complexities, the rotational barrier was reported to range from ~1.5 to ~3.0 kcal mol^{-1} for the co-planar $PhOCH_3$ and from ~0.5 to ~1.4 kcal mol^{-1} for the orthogonal $PhOCF_3$.[1a,9] Results from experimental studies of anisole disagreed on the exact magnitude of the barrier height in gas phase, but they generally estimated it as $<$3.1 kcal mol^{-1}.[9b] Overall, the dramatic effects of fluorine on ligand conformational bias could clearly influence ligand binding affinities and should be an important consideration when exploring fluoroanisoles as potential anisole bioisosteres.

Comparison of properties

Each replacement of hydrogen with fluorine results in an increase of 18 in molecular weight. The Clog*P* increment is nevertheless nonlinear. The first and second fluorine add 0.17 and 0.27 log units each, while the last fluorination dramatically increases Clog*P* by 0.66 in value. As a result, the OCH_3 to OCF_3 conversion is associated with an increase of 54 in molecular weight and 1.1 log units in Clog*P* (Figure S3).

Matched molecular pair analysis using the Pfizer compound collection yielded 700 $PhOCH_3$ and $PhOCF_3$ pairs, 217 $PhOCF_2H$ and $PhOCH_3$ pairs, and 213 $PhOCF_2H$ and $PhOCF_3$ pairs. For each pair, we mined experimental data for differences in physicochemical and ADME properties, with a goal to develop a better understanding for the generality of the observed trends. Such knowledge could help us make more rational choices in compound design with respect to introducing fluorine atoms.

To better illustrate trends for the relatively large number of data points in the HLM and RRCK data sets, we applied classification guidelines recommended by Pfizer PDM (Pharmacokinetics, Dynamics and Metabolism) scientists for characterizing compounds. Based on studies of standards with known in vivo hepatic extraction and back calculation from 0.3 and 0.7 in vivo extraction ratios, an HLM clearance of $<$9.2 μL min^{-1} mg^{-1} is considered low, and $>$48 μL min^{-1} mg^{-1} is deemed high clearance. Clearance values in between are regarded moderate. Similarly, three classification ranges were recommended to provide guidance for project teams on absorption potential of compounds: low, moderate, and high absorption using 2.5 and 10×10^{-6} cm s^{-1} of RRCK values. These thresholds are derived based on studies of standards with known in vivo absorption values and transport mechanisms, and taking into account the experimental variations.[10]

Comparison of anisoles and trifluoroanisoles

Lipophilicity: log D

Lipophilicity has been shown to significantly impact binding affinity, pharmacokinetics and toxicity.[11] Highly lipophilic compounds tend to afford low solubility and poor metabolic stability, leading to low oral bioavailability.[12] High lipophilicity is also frequently associated with increased promiscuity, giving rise to higher risk of adverse events.[13] Over the years, lipophilicity has been recognized as a key drug-like physicochemical property that determines the overall quality of a clinical candidate.[11b,14] A recent report has revealed a marked increase in the lipophilicity of compounds being synthesized in leading pharmaceutical companies.[11b] Efforts to reverse this trend are needed to decrease attrition in drug discovery and development due to lack of selectivity and compound-related toxicological events.

Clog*P* calculation is the most widely used assessment for lipophilicity of a compound.[15] However, for molecules that contain charged moieties it does not take into account the proper ionic states and their influence on partitioning into aqueous and hydrophobic (e.g., octanol) phases. The distribution coefficient (log*D*) addresses this by taking into account the extent of ionization at a certain pH and the distribution between the two immiscible solutions at equilibrium.

The idea of MMP analysis is to systematically identify pairs of molecules with minor structural differences and determine the associated property changes. A pairwise plot of log*D* values relating to the OCH_3 to OCF_3 transformation is shown in Figure 4. The strong impact on log*D* is evidenced by the predominantly higher values of OCF_3 compounds than their OCH_3 matched molecular pairs. Except for three outliers (out of thirty), triple fluorination adds lipophilicity to the anisole, causing an incremental change anywhere between 0.3 and 1.3 log units. This is in keeping with a recent comparative analysis reporting an increase of 1 log*P* unit upon replacement of an OCH_3 by the OCF_3 group.[16] One of the outliers, where the OCH_3 (log*D*: 3.63) was reportedly more lipophilic than the OCF_3 (log*D*: 3.21) compound, was in rather high log*D* space where the experimental measurements can be less reliable. On average, the replacement of OCH_3 by OCF_3 leads to a clear increase in log*D* which corroborates the prediction from the calculated Clog*P* values. This compelling trend could predispose the compound into a higher lipophilicity space leading to detrimental effects in drug-like properties.

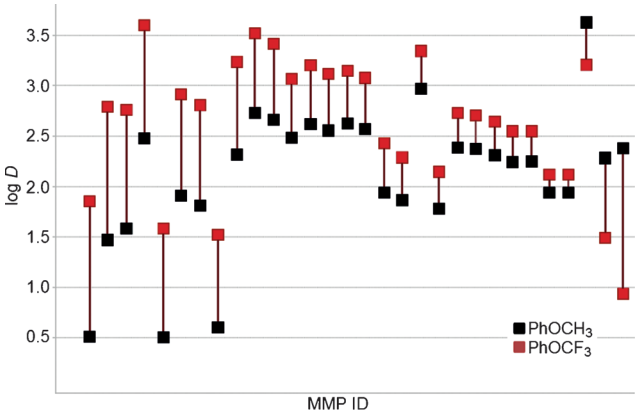

Figure 4. Experimental log*D* values for the OCH_3 and OCF_3 MMPs. Except for very few pairs, the OCF_3 compounds are predominantly more lipophilic by 0.3–1.3 log units than their OCH_3 analogues.

Metabolic stability

Metabolic stability is an important component of the ADME profile of a compound that needs to be balanced with target potency. Low metabolic stability is associated with issues such as high hepatic clearance, short half-life, poor in vivo exposure and lack of efficacy. In a lead optimization campaign, a frequently employed strategy to improve metabolic stability is to block enzymatic oxidation by replacing hydrogens with fluorine atoms at the reactive positions.[6] While such a strategy effectively circumvents the site-specific CYP-mediated metabolism, it can have the overall effect of increasing the lipophilicity of the molecule, which in turn could result in deterioration of metabolic stability due to enhanced binding to the target liver enzymes. The net result of the two competing trends is not always clear. Herein we compare the clearance data measured in human liver microsomes (HLM) for anisoles and fluoroanisoles to investigate if trends exist in the matched molecular pairs.

A total of 439 MMPs were identified which have been tested in the HLM assay. Figure 5 plots the experimental HLM clearance ($\mu L\,min^{-1}\,mg^{-1}$) for all the matched molecular pairs of $PhOCH_3$ and $PhOCF_3$ compounds. In the scatter plot (Figure 5a) it is noted that the distributions of the HLM clearance appear largely the same for the OCH_3 and OCF_3 compounds. No clear advantage of OCF_3 over OCH_3 is manifested. The lack of advantage in HLM is further illustrated in the histogram of Figure 5b, where the MMPs are binned by their measured microsomal clearance in three categories: stable (HLM < 9.2), moderate and unstable (HLM > 48). In the bar chart, the number of OCF_3 analogues is only marginally higher than the number of OCH_3 analogues amongst compounds of high stability (92 vs. 83), and is lower amongst compounds of low sta-

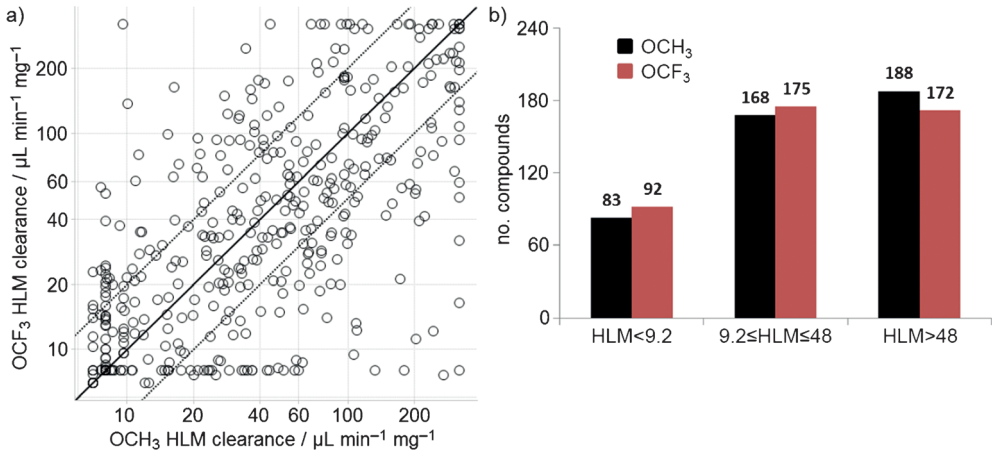

Figure 5. Experimental HLM clearance for the OCH_3 and OCF_3 MMPs. a) Each data point in the scatter plot represents one MMP. Replacement of OCF_3 shows no clear advantage over OCH_3 in terms of metabolic stability. Dotted lines delineate twofold boundaries around the diagonal. b) In the histogram, OCF_3 shows a slightly greater number of stable compounds (HLM < 9.2) and fewer unstable compounds (HLM > 48) by a very small margin (9–11%). The Wilcoxon signed-rank test indicates that there is no statistically significant HLM difference between the OCH_3 and OCF_3 MMPs ($p = 0.09$).

bility (172 vs. 188), but the differences are merely 9–11%. The Wilcoxon signed-rank test indicates that, for the given data set, the HLM differences between the OCH_3 and OCF_3 compounds are not statistically significant ($p = 0.09$). It is intriguing to observe that blocking all three hydrogen atoms that are potential substrates of oxidative metabolism by incorporating fluorine atoms does not, on average, alter HLM clearance to an appreciable extent. The reason could be either the OCH_3 is not the major site of metabolism, or the metabolism migrates to other parts of the molecule after OCF_3 installation. Overall, the data here suggest that there is, on average, no compelling advantage of OCF_3 over OCH_3 for designing more stable compounds.

There is a strong compound-specific characteristic to the impact of swapping OCH_3 for OCF_3 on metabolic stability. Many compounds display dramatic increases in stability upon incorporation of OCF_3, for example, 52 MMPs migrated from either low or medium buckets to high metabolic stability; however, a similar number of compounds (39 MMPs) display similarly dramatic decreases in stability upon the same conversion, falling from either stable or moderately stable categories to unstable. This could happen when the ether moiety is only one of the major sites for metabolism, and/or the tangible increase in lipophilicity by fluorination enhances binding to CYP enzymes, which could cause more rapid metabolism of the other parts of the molecules. In summary, the OCH_3 to OCF_3 modification is not a universal fix for metabolic stability; additionally, due to considerable addition of molecular weight (+54) as well as lipophilicity (+1.1 log unit), other drug-like properties could deteriorate.

RRCK permeability

Among the various ADME properties, permeability has been widely recognized as an important property of drug candidates. It plays a critical role in oral absorption, blood-brain barrier permeation, cell-membrane penetration for intracellular targets and skin absorption of transdermal products.[17] Permeability also has significant impact on metabolism and transporter effects, drug disposition and pharmacokinetics–pharmacodynamics relationships.[18] Along with other biopharmaceutical properties, permeability is an important determinant to the success of drug candidates in the clinic.

Passive permeability values measured in the RRCK cell line for 172 OCH_3 and OCF_3 MMPs are plotted in Figure 6. The pie charts are binned by Clog*P* values (Figure 6a). It is interesting that, as Clog*P* increases from 1 to 5, the percentages of the permeable compounds as measured by RRCK decreases. Indeed, for extremely high lipophilicity, for example, Clog$P > 5$, very few compounds show passive permeability in RRCK (<10%). The optimal range appears to be $1 < \text{Clog}P < 3$, in which the fractions of permeable compounds are the highest for both the OCH_3 and the OCF_3 groups (~70%). However, the apparently low permeability seen at the high Clog*P* range should be treated with caution, as this could potentially be an artifact of the RRCK assay, reflecting depoting of compounds in the cell membrane and/or solubility issues.

The impact of fluorination on the RRCK permeability is also revealed by the distribution histogram in Figure 6b. It is shown that the OCH_3 compounds are more enriched in the high permeability bucket (105 vs. 72, 46% enrichment) than the OCF_3 analogues, and less populated in the low permeability bucket (29 vs. 51, 76% reduction). The Wilcoxon signed-rank test produced a significant *p* value of 1×10^{-9}, suggesting that there is a strong RRCK difference between the OCH_3 and OCF_3 MMPs. Pairwise comparison of OCH_3 and OCF_3 compounds indicates that in ~70% of the total MMPs, the anisole is more permeable than the trifluoroanisole (104 out of 150). Due to the extended bond lengths of the C-F moiety and the larger van der Waals radii of a fluorine atom, the CF_3 group is considerably larger in dimensions than the CH_3, carrying approximately twice the volume. The larger molecular size may be deleterious to membrane penetration via a trans-cellular route, potentially rendering the OCF_3 group intrinsically less permeable than the parent OCH_3 group.

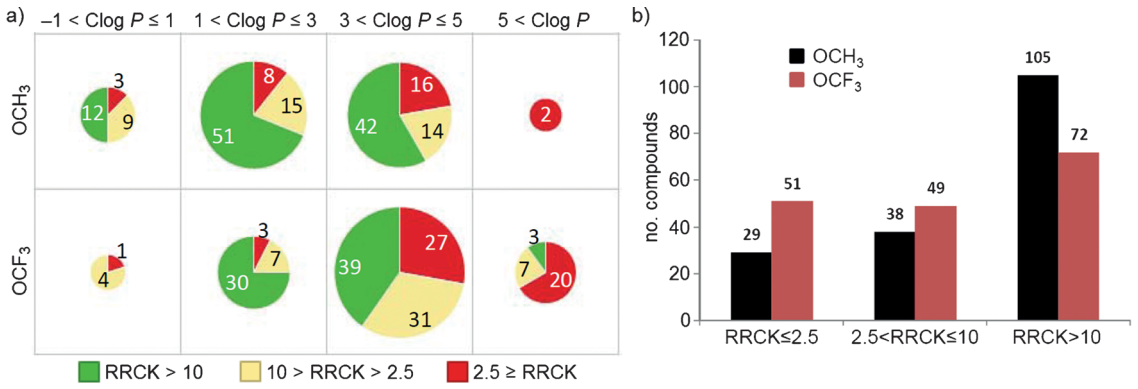

Figure 6. Experimental RRCK permeability [10^{-6} cm s^{-1}] for the OCH_3 and OCF_3 MMPs. a) Pie chart of permeability for OCH_3 and OCF_3 matched molecular pairs, binned by Clog*P* values as indicated in green, yellow, and red. Values denote the number of compounds in each pie graph. There are shifts into higher Clog*P* bins as OCH_3 is replaced by OCF_3, but OCF_3 compounds display poorer RRCK properties despite their higher Clog*P* values. b) In the histogram, OCH_3 shows one third of OCF_3 compounds in the poor permeability bin (RRCK ≤ 2.5), and 46% more compounds in the high permeability bin (RRCK > 10). The numbers of compounds in the medium permeability bin are similar for OCH_3 and OCF_3. The Wilcoxon signed-rank test indicates a strong RRCK difference between the OCH_3 and OCF_3 MMPs ($p = 1 \times 10^{-9}$).

In summary, it is demonstrated that the $PhOCH_3$ to $PhOCF_3$ modification is often associated with higher log*D* and lower cellular permeability. Although such a transformation is usually prompted by a desire to improve metabolic stability of a compound, our data suggests this strategy yields very mixed outcomes. These results intrigued us to take a close look at $PhOCF_2H$ in search for a better option of $PhOCH_3$ replacement.

Comparison of difluoroanisoles and trifluoroanisoles

*Lipophilicity: log*D

Pairwise plots for log*D* values relating to the OCF_2H to OCF_3 transformation are shown in Figure 7a. In almost all cases, OCF_3 is more lipophilic than OCF_2H. Except for one major outlier, there is typically an addition of 0.3–0.7 log units to log*D* values for the OCF_2H to OCF_3 transformation. In agreement, Müller has reported an increase of ~0.7 log*P* units for the same conversion.[16] The exception where OCF_2H (log*D*: 4.86) was reportedly more lipophilic than OCF_3 (log*D*: 3.87) was in very high log*D* space where experimental measurements can be unreliable. On average, the addition of the third fluorine atom yields a further increase in lipophilicity, which could lead to detrimental effects in drug-like properties.

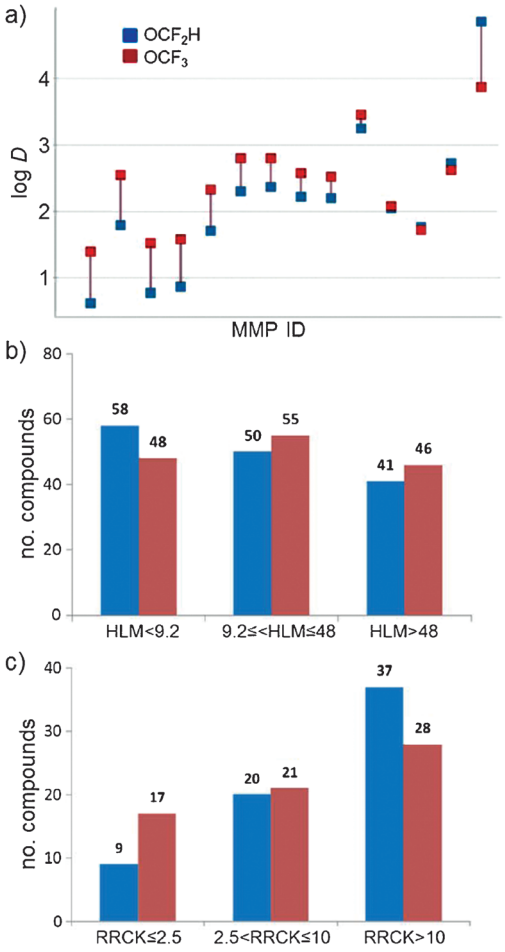

Figure 7. Comparisons of OCF_2H and OCF_3 MMPs. a) Experimental log*D* values. Except for very few pairs, OCF_3 compounds are predominantly more lipophilic by 0.3–0.7 log units than their OCF_2H analogues. b) Histogram of experimental HLM clearance. OCF_2H show a slightly larger fraction of stable compounds (HLM < 9.2), and a smaller fraction of unstable compounds (HLM > 48) than OCF_3. The Wilcoxon signed-rank test suggests OCF_2H compounds are significantly more stable than their OCF_3 MMPs ($p = 0.02$). c) Histogram of experimental RRCK permeability. OCF_2H shows half of the numbers in the poor permeability bin (RRCK ≤ 2.5), and 32% more compounds in the high permeability bin (RRCK > 10). The numbers of compounds in the medium permeability bin are similar for OCF_2H and OCF_3. The Wilcoxon signed-rank test indicates that there is a significant RRCK difference between the OCF_2H and OCF_3 MMPs ($p = 0.008$).

Metabolic stability

There are in total 149 MMPs of OCF_2H and OCF_3 compounds with the experimental HLM clearance data. Some compounds are slowly metabolized and do not have detectable turnover in the HLM assay, reaching the lower assay limit of 7 $\mu L\,min^{-1}\,mg^{-1}$. At the other end of the spectrum, for compounds that are extremely rapidly metabolized, their clearance values are flagged as greater than 320 $\mu L\,min^{-1}\,mg^{-1}$. Due to such detection limits at the ceiling and the floor of the assay, 32 pairs showed the same HLM clearances for the underlying analogues. In the remaining 117 pairs, more than half (67 out of 117) of them exhibited that OCF_2H has higher metabolic stability, or lower clearance, than their corresponding OCF_3 counterparts. In eight pairs of OCF_2H to OCF_3 conversions the metabolic stability decreased from medium to low, whereas there is only one case where the change improved HLM stability from low to medium. More examples are found where matched analogues move between medium and high stability tiers. For such transformations, OCF_3 is favored in seven instances, whereas OCF_2H is preferred in fifteen examples where the compounds are promoted to high stability category from their corresponding OCF_3 analogues of medium stability. In two extreme cases the OCF_2H compounds are metabolically stable (HLM < 9.2) while their corresponding OCF_3 strict pairs are unstable (HLM > 48). Therefore, examples suggest that the outcomes of OCF_2H to OCF_3 change are compound specific. Moreover, there is, on average, a small advantage of OCF_2H over OCF_3 with respect to rectifying metabolic stability. This is likely due to the decreased molecular lipophilicity of OCF_2H compounds which could attenuate the overall binding affinity to the CYP enzymes. Histograms of the number of compounds in different metabolic stability bins demonstrate similar distribution patterns for OCF_2H and OCF_3 (Figure 7b): a total of 58 OCF_2H compounds are in the stable category, compared with 48 OCF_3 analogues. On the other hand, fewer OCF_2H compounds are in the unstable bucket (41 OCF_2H vs. 46 OCF_3), as well as in the moderate stability group (50 OCF_2H vs. 55 OCF_3). The Wilcoxon signed-rank test on pairwise data yielded a significant HLM difference ($p = 0.02$). Therefore, contrary to the general practice of replacing hydrogens with fluorine atoms to block metabolic degradation, evidence supports that OCF_3 shows no improvement but possibly a slight decline in metabolic stability over OCF_2H analogues.

RRCK permeability

Passive permeability values measured in the RRCK cell line are analyzed for OCF_2H and OCF_3 pairs. In the majority of the matched pairs, the OCF_2H compounds display higher permeability than their OCF_3 analogues. Specifically, out of the 66 total pairs, 44 (67%) showed improvement of OCF_2H over OCF_3. The magnitude of improvements typically varies between 5 and 10×10^{-6} cm s^{-1}, and sometimes can be as high as more than 20×10^{-6} cm s^{-1}. When the compounds are classified into different permeability buckets (Figure 7c), OCF_2H has half of the number of compounds in the low RRCK ($\leq$2.5) category relative to OCF_3 (9 vs. 17, specifically), and 32% more in the high permeability (RRCK > 10) group (37 vs. 28 compounds, specifically). The number of compounds of medium permeability (2.5 < RRCK $\leq$ 10) are about the same: 20 for OCF_2H and 21 for OCF_3 respectively. The Wilcoxon signed-rank test indicates that there is a significant RRCK difference between the OCF_2H and OCF_3 pairs ($p = 0.008$).

The CF_2H group has interesting characteristics. Due to its asymmetric substitution pattern, two distinct conformational states exist as discussed in the previous section. Both the *endo-endo* and *endo-exo* conformations have been observed in the CSD (Figure S2). Simplified bond vector analysis indicate that there is nearly cancellation of bond polarities in the *endo-endo* arrangement.[16] On the other hand, in the *endo-exo* conformation the polarity of OCF_2H group is three times that of the *endo-endo* state. As a result, while the *endo-exo* state is more polar than the OCF_3 group ($\Delta\log P \sim -0.8$), the *endo-endo* conformation is equally or even slightly more lipophilic ($\Delta\log P \sim +0.1$) than the OCF_3 group.[16] In the lipid environment the OCF_2H group is expected to preferentially adopt the *endo*-endo conformation, which could explain the improved cellular permeability over the OCF_3 compounds. Conversely, the more polar *endo-exo* conformation may predominate in the aqueous solution, giving rise to the downshift of half a log *D* unit on average from the OCF_3 compounds. An earlier MMP analysis of neutral pairs reported the same findings on log *P* trend.[16]

In summary, OCF_2H compounds are less lipophilic than OCF_3. There is also a statistical advantage of OCF_2H compounds over their OCF_3 direct analogues to deliver superior transmembrane permeability and similar-to-better HLM stabilities.

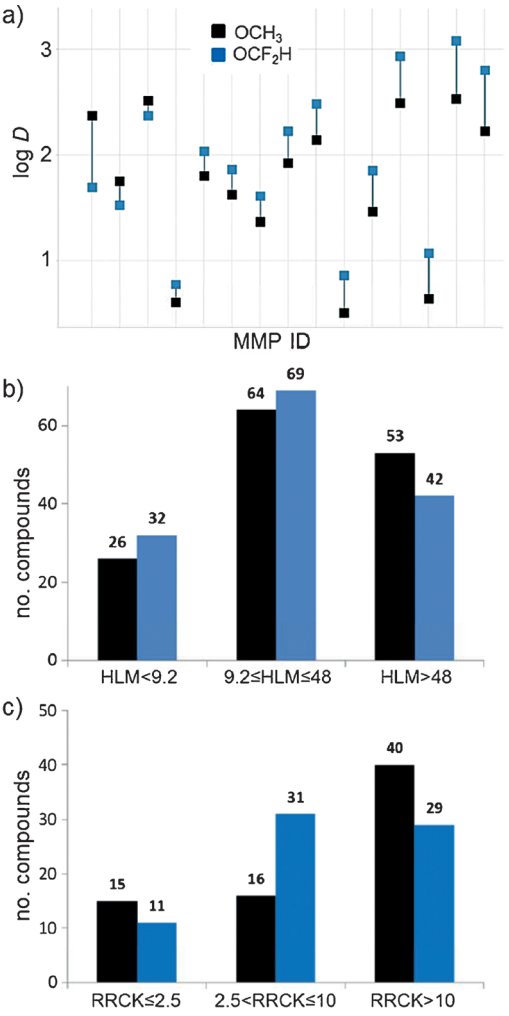

Figure 8. Comparisons of OCH_3 and OCF_2H MMPs. a) Experimental log *D* values. Except for very few pairs, OCF_2H compounds are more lipophilic by 0.2–0.6 log units than their OCH_3 analogues. b) Histogram of experimental HLM clearance. OCF_2H shows a larger fraction of stable compounds (HLM < 9.2), and a smaller fraction of unstable compounds (HLM > 48) than OCH_3. The number of compounds of medium HLM is also higher for OCF_2H than for OCH_3. The Wilcoxon signed-rank test indicates that the OCF_2H compounds are significantly more stable in HLM assay than their OCH_3 MMPs ($p = 0.01$). c) Histogram of experimental RRCK permeability. OCF_2H shows a smaller fraction of highly permeable compounds (RRCK > 10), and a larger fraction of moderate permeability (2.5 < RRCK $\leq$ 10) than OCH_3. The combined numbers of permeable compounds (RRCK > 2.5) are similar for OCF_2H (60) and OCH_3 (56).

Comparison of anisoles and difluoroanisoles

We have also generated OCF_2H versus OCH_3 data set to complete the analysis. In Figure 8a the experimental log *D* values are plotted for the corresponding MMPs. In general the OCF_2H compounds are more lipophilic than their OCH_3 analogues by 0.2–0.6 log units. This agrees with a separate analysis reporting an increase of 0.3 log *P* unit from OCH_3 to OCF_2H.[16] A histogram of experimental HLM clearance is depicted in Figure 8b. More OCF_2H compounds are in the metabolically stable category than the OCH_3 analogues (32 vs. 26), and fewer are in the unstable category (42 vs. 53). More OCF_2H compounds also show moderate stability than OCH_3 analogues (69 vs. 64). The Wilcoxon signed-rank test indicates that there is a significant HLM difference between the OCF_2H and OCH_3 MMPs ($p = 0.01$). The advantage of OCF_2H over OCH_3 in terms of HLM stability is also evidenced by the pairwise and scatter plots in the Supporting Information (Figure S8). Analysis of the RRCK MMPs (Figure 8c) indicates a slight decrease in numbers of OCF_2H versus OCH_3 compounds in the low (RRCK $\leq$ 2.5) and high RRCK bin (> 10). In general the OCH_3 compounds are more permeable than their OCF_2H MMPs. The Wilcoxon signed-rank test comparing the pairs produced a significant *p* value of 0.009. In the more permeable ranges (RRCK > 2.5) the numbers of compounds are largely similar for OCF_2H and OCH_3 (60 vs.

56). Similar numbers of OCF_2H and OCH_3 compounds appear in the low permeability range (11 vs. 15). Therefore, despite the increase in log *D*, statistical trends suggest that OCF_2H may improve upon OCH_3 in terms of HLM. While RRCK may be modestly compromised relative to OCH_3, OCF_2H is significantly better than OCF_3 in this respect (Figure 7C).

To summarize, results from our systematic MMP analysis using data from the Pfizer corporate database recommend OCF_2H as a more suitable option than OCF_3 to replace OCH_3 in medicinal chemistry optimization. Fluorination of anisole adds lipophilicity to the molecules, with a monotonic increase in experimental log *D* from OCH_3 to OCF_2H to OCF_3. The trifluoromethyl anisoles are substantially more lipophilic than the parent anisoles, with a typical elevation between 0.3 and 1.3 log units in the log *D* values. Bearing a good balance of molecular weight and lipophilicity, the OCF_2H moiety can deliver improvement in metabolic stability without notably compromising transcellular absorption.

Synthetic approaches

Although the use of fluorine in drug design is a common medicinal chemistry maneuver, introduction of fluorine into drug-like molecules can prove challenging. In the context of the analysis presented herein, we will now discuss synthetic approaches to fluoroanisoles and their relative synthetic accessibility.

Difluoromethoxy derivatives are typically generated from the phenol and difluorocarbene.[19] Generation of the difluorocarbene can be achieved via a number of different methods including decarboxylative methods, base mediated α-elimination and nucleophile-mediated α-elimination (Scheme 1).

The use of chlorodifluoromethane[20] and base represents the most obvious method of formation of difluoromethoxy derivatives. The reaction occurs via α-elimination of HCl from the chlorodifluoromethane and therefore requires strongly basic conditions although it does occur at low temperatures. The main disadvantages of the method are the use of an ozone depleting reagent, the strongly basic conditions and the fact that ClF_2CH is a gas. These requirements decrease the value of this approach on scale. However, Hartwig[21] has recently built on this approach by using difluoromethyltriflate, which is a non-ozone-depleting liquid. Reaction with difluoromethyltriflate typically occurs in minutes at room temperature and the method looks to hold some promise (Scheme 2).

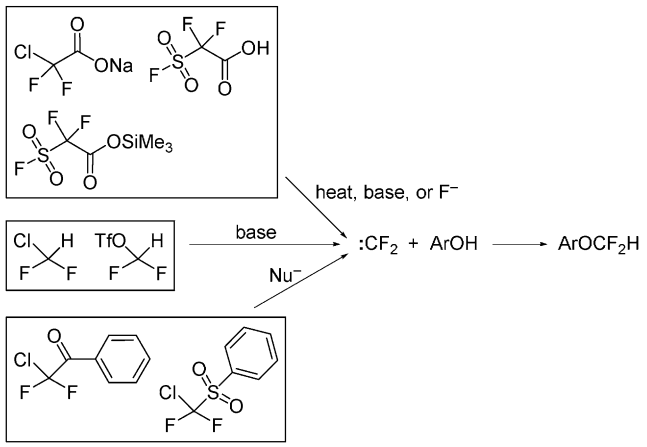

Scheme 1. General routes for the formation of difluoromethoxy derivatives.

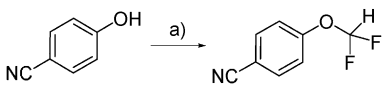

Scheme 2. *Reagents and conditions:* a) HCF_2OTf, KOH, CH_3CN/H_2O (1:1), RT, 2 min, 88%.

α-Elimination can also be triggered by attack on a carbonyl[22] or sulfonyl group[23] using a suitable nucleophile (Scheme 3) although these methods have been used less frequently.

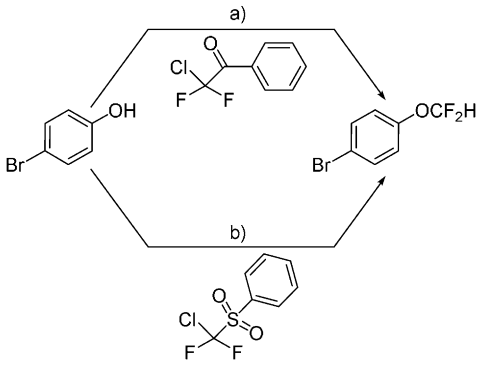

Scheme 3. *Reagents and conditions:* a) KOH, CH_3CN/H_2O (1:1), 80 °C, 4 h, 66%; b) KOH, CH_3CN/H_2O (7:2), 50 °C, 4 h, 74%.

In terms of methods deployed in the pharmaceutical industry, it is the decarboxylative methods that are most commonly used. Pyrolysis of sodium chlorodifluoroacetate ($ClCF_2CO_2Na$) occurs on heating to give the difluorocarbene[24] which reacts with phenols under basic conditions to give difluoromethoxyaryl derivatives. While the main limitation of this method is the requirement for high temperatures, the method has a number of advantages including the ready availability of sodium chlorodifluoroacetate and the scalability of the reaction. For example, this method has been used successfully on scale by Wyeth (Scheme 4) for the synthesis of a mGlurR5 negative allosteric modulator.[25] Use of potassium carbonate in DMF at 95 °C allowed the reaction to proceed in excellent yield on multi-kilogram scale.

While the pyrolysis of sodium chlorodifluoroacetate requires elevated temperatures to generate the difluorocarbene, the pyrolysis of 2-(fluorosulfonyl) acetic acid[26] can be achieved at

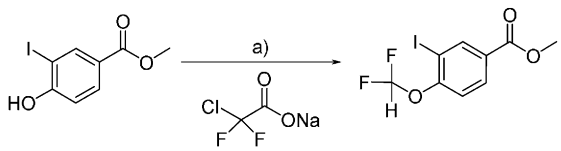

Scheme 4. *Reagents and conditions:* a) DMF, K_2CO_3, 95 °C, 4 h, 99.7%.

much lower temperatures which can be advantageous in some circumstances. For example, in their work on CRF antagonists, BMS found that a 2-difluoromethoxypyridine derivative could be generated from a nitropyridone at room temperature under basic conditions using 2-(fluorosulfonyl) acetic acid or its silylated variant[27] and occurred in excellent yield (Scheme 5).

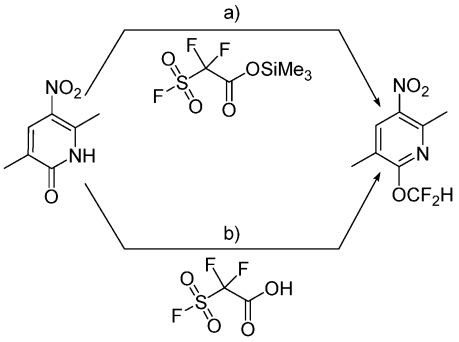

Scheme 5. *Reagents and conditions:* a) NaH, CsF, CH_3CN, RT, 70 min, 92%; b) NaH, CH_3CN, RT, 15 min, 96%.

Notably, the authors found that the use of chlorodifluoroacetate gave lower and more variable yields. This observation is consistent with in-house work at Pfizer where the 2-(fluorosulfonyl)acetic acid derivatives have often proven more effective for more sensitive substrates. Importantly, this method is also scalable and the intermediate was synthesized on multi-kilogram scale[28] (Scheme 6).

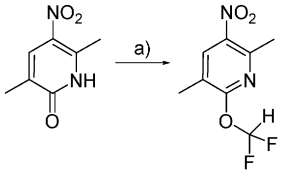

Scheme 6. *Reagents and conditions:* a) $FSO_2CF_2CO_2H$, NaH, CH_3CN, 10 °C, 3 h, 86%.

It is instructive to compare the synthesis of difluoromethoxy aromatics with trifluoromethoxy aromatic derivatives. Trifluoromethoxy aromatics are typically accessed by formation of the trichloromethoxy aromatic and then displacement of the chlorines by fluorines;[29] this reaction typically requires strongly acidic conditions and can be done with hydrogen fluoride or a mixture of antimony trifluoride and antimony pentachloride which is used as a melt. This conversion can be quite challenging and sensitive motifs are unlikely to survive. For example, while 2-pyridones can be readily converted into 2-difluoromethoxypyridines in one step[30] by using the methods we have previously detailed (with the difluorocarbene preferentially reacting at oxygen), the conversion of 2-pyridones to 2-trifluoromethoxypyridine derivatives is more challenging; in fact, a search of the literature suggests that only the 6-chloro variant is known (Scheme 7).[29a] This is consistent with in-house experience at Pfizer which suggests that the conversion of the

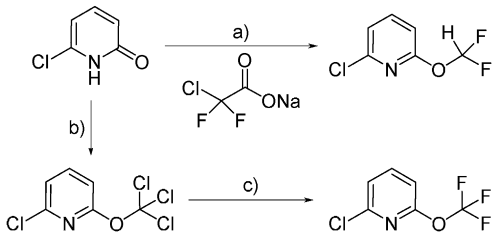

Scheme 7. *Reagents and conditions:* a) NaOH, H_2O, DMF, 55 °C, 18 h, 53%; b) 1. $CSCl_2$, NaOH, H_2O, $CHCl_3$, 0 °C, 2 h, 2. Cl_2, $CHCl_3$, 25 °C, 24 h, 60%; c) SbF_3, $SbCl_5$, 140 °C, 3 h, 53%.

2-trichloromethoxy pyridine to a 2-trifluoromethoxy pyridine derivative is quite challenging under the strongly acidic conditions and it is possible that the pyridone is regenerated instead. While a coupling protocol has recently been developed for trifluoromethoxy aromatics,[31] it does not work with pyridyl derivatives and novel methods accessing trifluoromethoxy derivatives are still highly desirable.

If we turn to monofluoromethoxy derivatives, it is striking that no 2-monofluoromethoxypyridine derivatives are known in the literature; this is consistent with the fact that this motif has been used much less frequently than the difluoro and trifluoromethoxy variants. Methods to make monofluoromethoxy aromatics[29b] include the use of chlorofluoromethane[32] and reaction with chloromethyl methyl thioether under basic conditions followed by reaction with xenon difluoride (Scheme 8).[33]

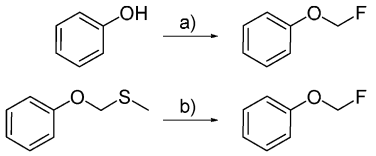

Scheme 8. *Reagents and conditions:* a) CH_2FCl, NaH, DMF, 80 °C, 3 h, 86%; b) XeF_2, $ClCH_2CH_2Cl$, 0 °C for 0.5 h then RT for 2 h, 80%.

Limited internal experience at Pfizer suggests that very low yields of the monofluoromethoxy aromatic are typically obtained using chloro- or bromo-fluoromethane. With the limited number of examples of this motif that are known, the question arises of whether the poor yields are down to the limitations of the synthetic methodology or to the stability issues with the motif. While instability issues have not been observed with difluoromethoxy and trifluoromethoxy aromatics, the extra fluorines present would presumably destabilize any oxonium species generated on expulsion of a fluoride (the acetal nature of all of these motifs would likely need to be invoked in any instability argument to demonstrate why the groups should have increased lability over a normal alkyl fluoride); for the monofluoromethoxy variant, expulsion of the fluoride would not lead to a destabilized oxonium species and the motif could therefore be viewed as having some lability; the ultimate stability would depend on how good a leaving group the fluoride was under the conditions used. With fluoride being a poor leaving group, this concern does seem unlikely to be an issue under physiological conditions; indeed, examination of the lit-

erature would suggest that the group is robust enough to survive a wide range of acidic and basic conditions. To get reaction to occur, the use of organolithium reagents or the presence of strong Lewis acids are typically required.[34] It therefore seems likely that limitations of the synthetic methodology have been the primary issue with the uptake of this motif; however, it would be fair to say that more work is needed to obtain a definitive position on its chemical stability.

Encouragingly, recent work by Chi using triazolium triflates suggests that good yields of monofluoromethoxy aromatics can be obtained.[35] Chi suggests that the intermediate triazolium triflate has very high reactivity with fluoride ions, possibly due to the ready formation of a zwitterionic carbene with the fluoride and that as a result, excellent yields of the desired product can be obtained. An example of the use of this methodology is shown in Scheme 9.[36]

The development of the triazolium triflate methodology is promising as, if it proves to have a wide scope, it may allow ready access to a range of monofluoromethoxyaromatics. It seems highly likely that if the stability concerns prove to be unfounded, this group will become increasingly popular in the pharmaceutical industry.

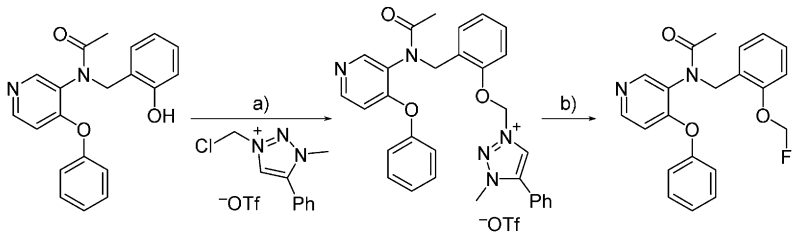

Scheme 9. *Reagents and conditions:* a) *t*BuOK, DMF, RT, 5 h, 35%; b) TBAF·3H_2O, CH_3CN, 80 °C, 1 h, 83%.

Conclusions

In summary, the matched molecular pair analysis described here demonstrates that anisole and fluoroanisoles have very different physicochemical and ADME properties in terms of lipophilicity, microsomal stability and cellular permeability. Trifluorination adds significant lipophilicity, and may compromise passive permeability. Importantly we find that trifluoroanisoles are not appreciably more metabolically stable than their methyl counterparts. The data suggests that difluoroanisoles may generally be a better alternative to trifluoroanisoles to address metabolic liabilities due to their lower lipophilicities and higher permeabilities. Although difluoroanisoles are under-explored relative to their trifluoroanisole counterparts, they are well-precedented in marketed drugs and several synthetic methods exist that provide ready access to the difluoroanisole moiety. An analysis of ligand conformation indicates that, whilst $PhOCH_3$ generally prefers the anticipated co-planar conformation, $PhOCF_3$ prefers a perpendicular orientation. In contrast, $PhOCF_2H$ appears to show a much less strong conformational bias and is thus unlikely to be 'locked' in an unproductive conformation that could preclude target binding. In conclusion, although OCF_3 is commonly explored as a replacement for OCH_3 in anisole-containing lead structures in order to optimize ADME properties, our analysis suggests OCF_2H may often prove a more attractive choice and greater exploitation of this motif is recommended.

Experimental Section

Conformational analysis: Conformational profiles of anisole and fluorinated anisoles were probed in the Cambridge Structural Database (CSD),[37] the repository of small molecule crystal structures. Substituents on the phenyl ring ortho to the alkoxy group could impact the conformational preferences of the ether by steric constraints. In order to avoid such bias, protons were explicitly drawn at one ortho position in the substructure queries to avoid steric forcing. In such a way we focused on the native conformational preferences of different fluorinated aryl ether groups with respect to the single bond connecting the oxygen and phenyl ring.

Computational retrieval of matched molecular pairs: In this study we focused on understanding the impact of the fluorination of aryl ethers to properties regarding lipophilicity, metabolic stability and permeability. The entire Pfizer compound collection was used as a source for the systematic retrieval of a comprehensive data set of matched molecular pairs (MMPs) of $PhOCH_3$, $PhOCFH_2$, $PhOCF_2H$ and $PhOCF_3$. The exact matched pairs are defined as pairs of molecules that differ only by fluorine replacements of protons on the methoxy group. The remaining parts of the molecules are identical within a matched pair. The experimental lipophilicity ($\log D$) values and ADME properties including permeability from Ralph Russ canine kidney (RRCK) cell line and human liver microsomal (HLM) clearance were retrieved from the Pfizer research informatics database.

A query-based approach was undertaken to perform the MMP analysis. A substructure search of $PhOCF_3$ in the corporate compound file yielded fifty thousand compounds. In the subsequent step, each $PhOCF_3$ containing molecule was transformed into the corresponding $PhOCF_2H$ and $PhOCH_3$ matched pairs using the Pipeline Pilot reaction processing function.[38] The SMILES strings for the transformed structures were standardized (canonicalized) and used to search the Pfizer corporate collection. This computationally efficient process identified 700 MMPs for the $PhOCH_3$ to $PhOCF_3$ transformation, 217 MMPs for the $PhOCH_3$ to $PhOCF_2H$ change, and 213 MMPs for the $PhOCF_2H$ to $PhOCF_3$ conversion. Only ten compounds were found containing $PhOCFH_2$ moiety, and very few had any experimental measurements. Given the small sample size that was insufficient to make statistical comparisons, the $PhOCFH_2$ substructure was not included in the analysis.

Data sets: The ADME and related properties, specifically $\log D$, HLM stability and RRCK permeability data were queried against the Pfizer research informatics database. For the $PhOCH_3$ to $PhOCF_3$ transformation, values for measured $\log D$ were retrieved for 30 pairs, HLM for 439 pairs, and RRCK permeability

for 172 pairs. For the $PhOCF_2H$ to $PhOCF_3$ conversion, there were available log *D* values for 14 pairs, HLM for 149 pairs, and RRCK for 66 pairs. And lastly for the $PhOCH_3$ to $PhOCF_2H$ transformation, 15 pairs for log *D*, 143 pairs for HLM and 71 pairs for RRCK were identified. The numbers of MMPs in each specific transformation are summarized in Table 1.

Table 1. Number of MMPs retrieved from the Pfizer corporate database.

	OCH_3 vs. OCF_3	OCH_3 vs. OCF_2H	OCF_2H vs. OCF_3
Total	700	217	213
log *D*	30	15	14
HLM	439	143	149
RRCK	172	71	66

The structural diversity of the compounds in the data set was analyzed using the $PhOCF_2H$ collection. When subjected to a nearest-neighbor analysis, the 213 compounds were found to cover different structural series of 45 clusters and 47 singletons, according to Ward's similarities (distance cutoff of 0.1) using CDK-Daylight fingerprints. The diverse representation of chemical classes attests the data set is not biased by any specific structural template, and the trends identified are generally applicable.

Experimental measurements: log *D*. Compounds were measured at pH 7.4 in octanol-water bilayer using shake flask method. DMSO stocks of compounds were mixed with octanol in equilibrium with buffer to provide a 1:1 (*v*/*v*) ratio. The concentrations of a compound being partitioned into both phases were measured by UV/Vis spectroscopy.

Human liver microsomal (HLM) stability. The high-throughput human microsomal stability assay was performed in a 384-well format. Pooled human liver microsomes were purchased from BD Biosciences (Bedford, MA). Each incubation contained test compound (1 μM), human liver microsomes (0.25 μM CYP protein equivalent to 0.71 mg mL^{-1} protein concentration), NADPH regenerating system (1 mM NADP+, 5 mM isocitric acid and 1 U mL^{-1} isocitric dehydrogenase), $MgCl_2$ (1 mM) and potassium phosphate buffer (100 mM at pH 7.4). The incubations were conducted at 37 °C. At various time points (0, 5, 10, 20, 30 and 60 min), cold acetonitrile with mass spectrometry (MS) internal standard (IS, CP-628374) was added to quench the reaction. The plates were centrifuged at 3000 rpm for 10 min at 4 °C (Sorvall RC 3C Plus, Thermo Scientific, Waltham, MA). The supernatant was transferred to a new 384-well plate, sealed and subsequently analyzed using LC–MS/MS.

Ralph Russ canine kidney (RRCK) permeability: The RRCK permeability assay (4-in-1 cassette dosing) is an in vitro high throughput assay of 96-well format.[10] The Ralph Russ Canine Kidney (RRCK) cells are a subpopulation of Madin–Darby canine kidney (MDCK) cells with low expression of endogenous canine P-gp transporter. The RRCK low-efflux cells were selected from MDCK-WT using an iterative fluorescence-activated cell sorting technique with calcein-AM as a P-gp and efflux substrate. The RRCK apparent permeability values differentiate compounds from high to medium/low human intestinal absorption and can be used for biopharmaceutical classification.

Statistical analysis: We performed statistical tests on the continuous MMP pairs. Because the RRCK and HLM data are not normally distributed a Wilcoxon signed-rank test is applied. The null hypothesis was that the population distributions in the corresponding pairwise groups (OCH_3 vs. OCF_3, OCF_2H vs. OCF_3 and OCH_3 vs. OCF_2H) are identical; a significant *p* value would lead to the rejection of the null hypothesis from which we could draw a conclusion that the data populations were different between the tested groups. A significance level of alpha$a = 0.05$ was used to control the false positive rate at 5% for each paired test of HLM and RRCK data set.

Supporting information: Structures of clinical candidates containing $PhOCF_2H$ moiety, CCDC examples ZIJFAB and SOTBAE, pairwise and scatter plots of HLM and RRCK for OCH_3 and OCF_3, OCF_2H and OCF_3, OCH_3 and OCF_2H MMPs, and Wilcoxon test statistics for log *D* differences between MMPs.

Abbreviations: MMP, matched molecular pair; CSD, Cambridge structural database; ADME, absorption, distribution, metabolism and excretion; CYP, cytochrome P450; HLM, human liver microsome; RRCK, Ralph Russ canine kidney.

Acknowledgements

We thank the peer reviewers for insightful suggestions. This study was sponsored by Pfizer Inc..

Keywords: ADME profiles · anisoles · drug design · fluorination · metabolic stability

[1] a) K. Muller, C. Faeh, F. Diederich, *Science* **2007**, *317*, 1881 – 1886; b) W. K. Hagmann, *J. Med. Chem.* **2008**, *51*, 4359 – 4369.
[2] C. Dalvit, C. Invernizzi, A. Vulpetti, *Chemistry* **2014**, *20*, 11058 – 11068.
[3] a) J. A. Olsen, D. W. Banner, P. Seiler, U. Obst-Sander, A. D'Arcy, M. Stihle, K. Muller, F. Diederich, *Angew. Chem. Int. Ed.* **2003**, *42*, 2507 – 2511; *Angew. Chem.* **2003**, *115*, 2611 – 2615; b) J. Olsen, P. Seiler, B. Wagner, H. Fischer, T. Tschopp, U. Obst-Sander, D. W. Banner, M. Kansy, K. Muller, F. Diederich, *Org. Biomol. Chem.* **2004**, *2*, 1339 – 1352; c) J. A. Olsen, D. W. Banner, P. Seiler, B. Wagner, T. Tschopp, U. Obst-Sander, M. Kansy, K. Muller, F. Diederich, *ChemBioChem* **2004**, *5*, 666 – 675.
[4] a) A. Vulpetti, N. Schiering, C. Dalvit, *Proteins Struct. Funct. Bioinf.* **2010**, *78*, 3281 – 3291; b) C. Dalvit, A. Vulpetti, *ChemMedChem* **2011**, *6*, 104 – 114.
[5] a) B. K. Park, N. R. Kitteringham, *Drug Metab. Rev.* **1994**, *26*, 605 – 643; b) B. K. Park, N. R. Kitteringham, P. M. O'Neill, *Annu. Rev. Pharmacol. Toxicol.* **2001**, *41*, 443 – 470; c) A. F. Stepan, V. Mascitti, K. Beaumont, A. S. Kalgutkar, *MedChemComm* **2013**, *4*, 631 – 652.
[6] H. J. Böhm, D. Banner, S. Bendels, M. Kansy, B. Kuhn, K. Muller, U. Obst-Sander, M. Stahl, *ChemBioChem* **2004**, *5*, 637 – 643.
[7] H. Sun, C. E. Keefer, D. O. Scott, *Drug Metab. Lett.* **2011**, *5*, 232 – 242.
[8] F. Leroux, P. Jeschke, M. Schlosser, *Chem. Rev.* **2005**, *105*, 827 – 856.
[9] a) S. Tsuzuki, H. Houjou, Y. Nagawa, K. Hiratani, *J. Phys. Chem. A* **2000**, *104*, 1332 – 1336; b) D. C. Spellmeyer, P. D. J. Gorootenhuis, M. D. Miller, L. F. Kuyper, P. A. Kollman, *J. Phys. Chem.* **1990**, *94*, 4483 – 4491.
[10] L. Di, C. Whitney-Pickett, J. P. Umland, H. Zhang, X. Zhang, D. F. Gebhard, Y. Lai, J. J. Federico III, R. E. Davidson, R. Smith, E. L. Reyner, C. Lee, B. Feng, C. Rotter, M. V. Varma, S. Kempshall, K. Fenner, A. F. El-Kattan, T. E. Liston, M. D. Troutman, *J. Pharm. Sci.* **2011**, *100*, 4974 – 4985.

[11] a) C. A. Lipinski, *J. Pharmacol. Toxicol. Methods* **2000**, *44*, 235 – 249; b) P. D. Leeson, B. Springthorpe, *Nat. Rev. Drug discovery* **2007**, *6*, 881 – 890.
[12] H. van de Waterbeemd, D. A. Smith, K. Beaumont, D. K. Walker, *J. Med. Chem.* **2001**, *44*, 1313 – 1333.
[13] K. Azzaoui, J. Hamon, B. Faller, S. Whitebread, E. Jacoby, A. Bender, J. L. Jenkins, L. Urban, *ChemMedChem* **2007**, *2*, 874 – 880.
[14] F. Giordanetto, J. Bostrom, C. Tyrchan, *Drug Discovery Today* **2011**, *16*, 722 – 732.
[15] C. Leo, C. Hansch, D. Elkins, *Chem. Rev.* **1971**, *71*, 525 – 616.
[16] K. Müller, *Chimia* **2014**, *68*, 356 – 362.
[17] E. H. Kerns, L. Di, *Drug-like Properties: Concepts, Structure Design and Methods: From ADME to Toxicity Optimization*, London, Elsevier, **2008**.
[18] a) C. Y. Wu, L. Z. Benet, *Pharm. Res.* **2005**, *22*, 11 – 23; b) D. A. Smith, *Curr. Top. Med. Chem.* **2011**, *11*, 467 – 481.
[19] D. L. Brahms, W. P. Dailey, *Chem. Rev.* **1996**, *96*, 1585 – 1632.
[20] a) A. Fuss, V. Koch, *Synthesis* **1990**, 604 – 608; b) A. Fuss, V. Koch, *Synthesis* **1990**, 681 – 685; c) B. R. Langlois, *J. Fluorine Chem.* **1988**, *41*, 247 – 261; d) T. G. Miller, *J. Org. Chem.* **1960**, *25*, 2009 – 2012.
[21] P. S. Fier, J. F. Hartwig, *Angew. Chem. Int. Ed.* **2013**, *52*, 2092 – 2095; *Angew. Chem.* **2013**, *125*, 2146 – 2149.
[22] L. Zhang, J. Zheng, J. Hu, *J. Org. Chem.* **2006**, *71*, 9845 – 9848.
[23] J. Zheng, Y. Li, L. Zhang, J. Hu, G. J. Meuzelaar, H. J. Federsel, *Chem. Commun.* **2007**, 5149 – 5151.
[24] a) D. Babin, F. Pilorge, L. M. Delbarre, J. P. Demoute, *Tetrahedron* **1995**, *51*, 9603 – 9610; b) L. H. Knox, E. Velarde, S. Berger, D. Cuadriello, P. W. Landis, A. D. Cross, *J. Am. Chem. Soc.* **1963**, *85*, 1851 – 1858.
[25] J. B. Sperry, R. M. Farr, M. Levent, M. Ghosh, S. M. Hoagland, R. J. Varsolona, K. Sutherland, *Org. Process Res. Dev.* **2012**, *16*, 1854 – 1860.
[26] Q.-Y. Chen, S.-W. Wu, *J. Fluorine Chem.* **1989**, *44*, 433 – 440.
[27] R. A. Hartz, V. T. Ahuja, X. Zhuo, R. J. Mattson, D. J. Denhart, J. A. Deskus, V. M. Vrudhula, S. Pan, J. L. Ditta, Y. Z. Shu, J. E. Grace, K. A. Lentz, S. Lelas, Y. W. Li, T. F. Molski, S. Krishnananthan, H. Wong, J. Qian-Cutrone, R. Schartman, R. Denton, N. J. Lodge, R. Zaczek, J. E. Macor, J. J. Bronson, *J. Med. Chem.* **2009**, *52*, 7653 – 7668.
[28] D. K. Leahy, J. Li, J. B. Sausker, J. Zhu, M. A. Fitzgerald, C. Lai, F. G. Buono, A. Braem, N. de Mas, Z. Manaloto, E. Lo, W. Merkl, B.-N. Su, Q. Gao, A. T. Ng, R. A. Hartz, *Org. Process Res. Dev.* **2010**, *14*, 1221 – 1228.
[29] a) B. Manteau, P. Genix, L. Brelot, J.-P. Vors, S. Pazenok, F. Giornal, C. Leuenberger, F. R. Leroux, *Eur. J. Org. Chem.* **2010**, 6043 – 6066; b) B. Manteau, S. Pazenok, J.-P. Vors, F. R. Leroux, *J. Fluorine Chem.* **2010**, *131*, 140 – 158.
[30] M. Burger, Y. Ding, W. Han, G. Nishiguchi, A. Rico, R. L. Simmons, A. R. Smith, J. V. Tamez, H. Tanner, L. Wan, *Tetrasubstituted Cyclohexyl Compounds as Kinase Inhibitors*, US Pat. No. US 2012225061 A1, **2012**.
[31] C. Huang, T. Liang, S. Harada, E. Lee, T. Ritter, *J. Am. Chem. Soc.* **2011**, *133*, 13308 – 13310.
[32] W. Zhang, L. Zhu, J. Hu, *Tetrahedron* **2007**, *63*, 10569 – 10575.
[33] Q. Lu, T. Benneche, *Acta Chem. Scand.* **1996**, *50*, 850 – 852.
[34] R. Ringom, T. Benneche, *Acta. Chem. Scand.* **1999**, *53*, 41 – 47.
[35] C. Park, B. S. Lee, D. Y. Chi, *Org Lett.* **2013**, *15*, 4346 – 4349.
[36] B. S. Moon, B. S. Kim, C. Park, J. H. Jung, Y. W. Lee, H. Y. Lee, D. Y. Chi, B. C. Lee, S. E. Kim, *Bioconjugate Chem.* **2014**, *25*, 442 – 450.
[37] The Cambridge Crystallographic Data Centre, Cambridge (UK): www.ccdc.cam.ac.uk.
[38] Pipeline Pilot ver. 8.5, Accelrys Inc.: www.accelrys.com.

Received: December 22, 2014
Revised: February 9, 2015
Published online on March 6, 2015